Analytical study and computer simulation of discrete optical breathers in a zigzag chain

L. I. Manevitch* and A. V. Savin†
N. N. Semenov Institute of Chemical Physics, Russian Academy of Sciences, ul. Kosygina 4, 119991 Moscow, Russia

C.-H. Lamarque‡
3, rue Maurice Audin, F69518 Vaulx-en-Velin Cedex, France

(Received 8 September 2005; revised manuscript received 26 May 2006; published 28 July 2006)

We present analytical and numerical studies of the discrete breathers identified as localized deformations of valence angles and bonds in crystalline polyethylene (PE). It is shown that such breathers can exist both outside and within the optical band and may propagate with subsonic velocities along the polymer chain. The analytical results are confirmed by numerical simulation using the molecular dynamics procedure. We examine also the stability of the breathers relative to thermal excitations and mutual collisions as well as to collisions with the acoustic nontopological and topological solitons. The conditions of the breathers existence depend strongly on their generating frequency, the relationship between the stiffness of valence bonds and valence angles as well as on the type of nonlinear characteristics of intrachain interactions.

DOI: 10.1103/PhysRevB.74.014305 PACS number(s): 63.20.Pw, 63.20.Ry, 05.45.−a

I. INTRODUCTION

In spite of growing interest to the study of localized nonlinear oscillatory excitations in solids, almost all activity in this field has been concentrated on the one-dimensional straight chains.[1,2] However, the realistic models of strongly anisotropic systems such as polymer crystals should take into account the zigzag or helix structure of the chains.

The two-dimensional linear dynamics of a planar zigzag chain was considered by Kirkwood[3] in application to polyethylene macromolecule more than 60 years ago. On the other side, the zigzag and helix chains can also be considered as discrete models of corrugated and spiral mechanical systems.[4] The studies of nonlinear dynamics of polymer chains and crystals in last decades have been lately stimulated by the possibility of numerous applications to such physical problems as dielectric relaxation,[5–7] premelting and melting,[8] heat conductivity,[9,10] polarization,[11] fracture,[12,13] plastic deformation,[14–17] DNA sequencing,[18] and so on. All mentioned applications are based on two types of solitons: supersonic solitons of tension and compression[12,19,20] as well as combined solitons of tension (compression) and torsion.[12,21–24]

In addition to these solitons, there are two examples of breathers in the models of polymer chains. The first one is a localized nonlinear vibration of C-H valence bond in the carbon-hydrogen chains. This breather appears due to anharmonicity of the corresponding potential;[25] the frequency of the breather ($\simeq$3100 cm^{-1}) is above that of the upper boundary of the lower optical branch of the IR spectrum. The second example is a localized periodic deformation of the valence angles and bonds in PE chains.[26] This breather has been revealed by numerical simulation. In this case the fundamental frequency ($\simeq$800 cm^{-1}) is close to the lower boundary of the first optical band for PE crystals. Due to this closeness, only one type of mobility corresponding to the transversal motion turned out to be predominant in the localization region of the breather. In addition only the stationary (nonpropagating) breathers have been found. Meanwhile, the valence angles potential for the PE chain[22] demonstrates the case when the lower frequency boundary of the optical band lies within the wave number range and far from its boundaries. This means that the possible breather has not a predominant component (longitudinal or transversal), hence the study becomes much more complicated than in Ref. 26.

In the present paper we remove both restrictions mentioned above and implying some closeness to the wave number boundary of the optical band and the stationarity of the breather, respectively. As this takes place, we present the first analytical description of the short wavelength nonlinear dynamics of the PE chain at all possible optical frequencies. This development goes beyond the earlier numerical simulation of the breathers.[26]

As for the present numerical study, in addition to thermal stability of the breathers we consider also their mutual collisions and collisions with the acoustic nontopological and topological solitons. It is worth mentioning that the interchain interaction does not affect significantly the optical breathers in the PE crystal (as opposed to topological solitons). Nevertheless, this interaction was considered in the course of numerical analysis.

The commonly studied breathers in the attenuation band are linearly stable. However, as it was shown in Ref. 26, the nonlinear interaction with the extended modes (thermal phonons) results in the relaxation of the breathers. Therefore, for the realistic models of polymer crystals there is no qualitative difference between the breathers in the attenuation and propagation bands, certainly if they exist in propagation band. On the other hand, the relaxation time is large enough and the breathers may have a significant effect on the different physical properties of PE crystal.[27]

At last, we would like to provide some guidance for the reader to keep track of the important equations (in the analytical part of the paper). We start from general nonlinear equations (4)–(7) of planar nonlinear dynamics of the zigzag chain. Then the modulating functions are introduced by expansions (12)–(15), and the relations (20)–(24) between these functions are found to derive Eqs. (25)–(28). Finally, complex equations of motion (30), (31), (45), and (46) cor-

 ©2006 The American Physical Society

responding to main asymptotic approximation have been obtained. So, rather complicated and lengthy calculations are necessary for derivation of final complex nonlinear Schrödinger-type equations (45) and (46). These equations provide the pass to the study of breatherlike nonlinear elementary excitations in strongly anisotropic crystals. As it is clear now, such excitations manifest themselves not only in heat capacity but also in heat conduction and premelting phenomena.[10,28]

II. DESCRIPTION OF THE MODEL

In the numerical study we take into account not only a planar motion of the chain, but also a spatial movement as well as interchain interactions. Therefore, the Hamiltonian presented below is three-dimensional one.

We suggest that the zig-zag initial structure of the PE macromolecule is directed along the z axis in the plane (x,z), while the y axis is perpendicular to the plane (x,z), so that (x,y,z) is the positive global reference of the problem and θ_0 is an angle of the zigzag chain.[26]

The initial coordinates of the nth mass of the chain are

$$z_n^0 = nl_z, \quad x_n^0 = (-1)^{n+1} l_x/2, \tag{1}$$

where $l_z = s\rho_0$ and $l_x = c\rho_0$ $[s=\sin(\theta_0/2), c=\cos(\theta_0/2)]$ are the longitudinal and transversal distances (respectively) between the carbon atoms in the initial zigzag chain. We use the approximation of "united atoms" because the relative motions of the hydrogen atoms are nonsignificant when dealing with a backbone deformation predominantly. So the magnitude of every mass is supposed to be equal to 14 a.u. Let us introduce the relative coordinates

$$u_n = x_n - x_n^0, \quad w_n = z_n - z_n^0, \tag{2}$$

where w_n, u_n, v_n determine respectively the longitudinal, transversal and out-of-plane displacements of the n th mass from its equilibrium state. Let us denote by ρ_n and θ_n the current length of the valence bond and current valence angle, respectively. We introduce also ϕ_n as the angle between d_{n-1} and the plane generated by d_n and d_{n+1} (the conformation angle).

The dynamics of the chain is governed by the following Hamilton function of the chain:[26]

$$H = \sum_{n=-\infty}^{+\infty} \left\{ \frac{1}{2} m(\dot{u}_n^2 + \dot{v}_n^2 + \dot{w}_n^2) + [p_1 + p_2\cos(\phi_n) + p_3\cos(3\phi_n)] + \frac{1}{2}\Lambda[\cos(\theta_n) - \cos(\theta_0)]^2 + \mathcal{D}[1 - e^{-q(\rho_n - \rho_0)}]^2 \right\} + Z(u_n, v_n, w_n), \tag{3}$$

where the overdots denote the time derivation. The first term in this expression is a kinetic energy. The next three ones correspond to the energy of conformation angles, valence angles, and valence bonds, respectively. The last term is the energy of interaction of the nth unit with six neighboring chains (the substrate potential) which are supposed to be immobile ones.

Parameters p_1, p_2, p_3 satisfy the conditions $p_1 = p_2 + p_3$, $p_2, p_3 > 0$, so that the undeformed state corresponds to the $\phi_n = \pi$. Let us set $k_1 = 2\mathcal{D}q^2$ and $k_2 = \Lambda\sin^2\theta_0$. The relations for ρ_n and θ_n are presented in Ref. 26.

The substrate potential:[26]

$$Z(u,v,w) = \varepsilon_w \sin^2(\pi w/l_z) + \frac{1}{2}K_u\left[1 + \varepsilon_u \sin^2\left(\frac{\pi w}{l_z}\right)\right] \times \left\{u - \frac{1}{2}l_x\left[1 - \cos\left(\frac{\pi w}{l_z}\right)\right]\right\}^2 + \frac{1}{2}K_v\left[1 + \varepsilon_v \sin^2\left(\frac{\pi w}{l_z}\right)\right]v^2,$$

where $\varepsilon_u = 0.0674265$ kJ/mol, $\varepsilon_v = 0.0418353$ kJ/mol, $\varepsilon_w = 0.1490124$ kJ/mol, $K_u = 2.169513$ kJ/Å mol^2, and $K_v = 13.683865$ kJ/Å mol^2.

III. PLANAR MOTION OF THE ZIGZAG CHAIN

In both linear and nonlinear problems the in-plane dynamics can be completely separated from the out-of-plane motion. Therefore, the Hamilton function for analytical study of the in-plane dynamics has to be simplified as follows:

$$H = \sum_{n=-\infty}^{+\infty} \frac{1}{2} m(\dot{u}_n^2 + \dot{w}_n^2) + \left\{ \sum_{n=-\infty}^{+\infty} \frac{1}{2}\Lambda[\cos(\theta_n) - \cos(\theta_0)]^2 + \sum_{n=-\infty}^{+\infty} \mathcal{D}[1 - e^{-q(\rho_n - \rho_0)}]^2 \right\}. \tag{4}$$

The PE macromolecules may be described by the two systems of parameters, which are introduced in Refs. 21 and 22, respectively. These systems differ by the parameter k_2 ($k_2/\sin^2\theta_0 = 130.1$ and 529 kJ/mol). We will consider both systems supposing that $k_1/q^2 = 334.7$ kJ/mol, $q = 19.1$ nm^{-1}, $\theta_0 = 113°$, $\rho_0 = 1.54$ Å so that $\delta = k_2/k_1\rho_0^2 = 0.019$ (see Ref. 21) or 0.078 (see Ref. 22).

The deformations are presented by their power series expansions up to second order terms:

$$\Delta\rho_n = \rho_n - \rho_0 = (u_n - u_{n+1})c + (w_{n+1} - w_n)s + \frac{1}{2\rho_0}[(u_n - u_{n+1})c + (w_{n+1} - w_n)s]^2 + \cdots, \tag{5}$$

$$\Delta\theta_n = \theta_n - \theta_0 = \frac{s}{\rho_0}(2u_n - u_{n-1} - u_{n+1}) + \frac{c}{\rho_0}(w_{n-1} - w_{n+1}) + \frac{cs}{\rho_0^2}[(u_n - u_{n+1})^2 + (u_n - u_{n-1})^2 - (w_n - w_{n+1})^2 - (w_n - w_{n-1})^2] + \frac{c^2 - s^2}{\rho_0^2}[(w_n - w_{n-1})(u_n - u_{n-1}) + (w_{n+1} - w_n)(u_n - u_{n+1})] + \cdots. \tag{6}$$

The equations of motion for the nth particle are

$$m\ddot{u}_n = -\frac{\partial H}{\partial u_n}, \quad m\ddot{w}_n = -\frac{\partial H}{\partial w_n}. \tag{7}$$

TABLE I. Values of Ω^2, ν, μ for some particular k.

k	Ω^2	ν	μ
0	$4s^2C_1$	0	$C_1[\cos(\theta_0)+4c^2\delta]$
π	$4C_1(c^2+4s^2\delta)$	0	$-C_1[\cos(\theta_0)c^2+20c^2s^2\delta/(c^2+4s^2\delta)]$
$\pi/2$	$2C_1$	$2C_1\cos(\theta_0)$	$4C_1C_2[\sin^2(\theta_0)/C1-2C_2]$

IV. DISPERSION RELATIONS

The linear dispersion curves have the well known form (see, e.g., Ref. 26):

$$\omega^2(k) = f(k) = \omega_0^2(k) \pm \sqrt{\omega_0^4(k) - \omega_1^4(k)}, \tag{8}$$

where

$$\omega_0^2(k) = C_1(1 - \cos\,\theta_0\cos\,k) + 2C_2(1 - \cos\,k) \times(1 + \cos\,k\,\cos\,\theta_0),$$

$$\omega_1^4(k) = 8C_1C_2(1 - \cos\,k)\sin^2 k. \tag{9}$$

Here $C_1=k_1/m$, $C_2=k_2/m\rho_0^2$, $k=\tilde{k}l_z$, where $\tilde{k}$ is the wave number. The "minus" and "plus" signs correspond to the acoustic and optical branches, respectively. We will consider further the optical branch only.

The asymptotic representation of the linear frequencies in the vicinity of an arbitrary wave number $k^\star$ can be presented as follows:

$$\omega^2(k) = \Omega^2 + \nu(k - k^\star) + \mu(k - k^\star)^2 + \cdots = f(k), \tag{10}$$

with

$$\Omega^2 = 2C_1[1 - \cos(\theta_0)\cos(k^\star)] - \frac{4C_2\cos^2(k^\star)\sin^2(\theta_0)}{1 - \cos(\theta_0)\cos(k^\star)} \times[1 - \cos(k^\star)],$$

$$\nu = 2C_1\sin(k^\star)\cos(\theta_0) + \frac{2C_2\sin(2k^\star)\sin^2(\theta_0)}{[1 - \cos(\theta_0)\cos(k^\star)]^2} \times\{[1 - \cos(k^\star)][2\cos(k^\star) - 1] + \cos(\theta_0)\cos(k^\star) - 1\},$$

$$\mu = C_1\cos(\theta_0)\cos(k^\star) + \frac{C_2\sin^2(\theta_0)}{[\cos(\theta_0)\cos(k^\star) - 1]^3} \times\{-4 + 12\cos(k^\star) + 4\cos^2(k^\star)[2 - 3\cos(\theta_0)] - 2\cos^3(k^\star)[-2\cos^2(\theta_0) + 3\cos(\theta_0) + 9] + 2\cos^4(k^\star) \times\cos(\theta_0)[\cos(\theta_0) + 11] - 8\cos^5(k^\star)\cos^2(\theta_0)\}. \tag{11}$$

Parameters ω^2, ν, and μ for several values of k are presented in Table I. Analysis of dispersion curves in application to realistic values of chain parameters reveals two types of behavior (Fig. 1). Let us introduce $C_2=\delta C_1$. The curvature $\mathcal{H}$ of optical dispersion curves is $\delta=0.019$, $\mathcal{H}(0)<0$, $\mathcal{H}(\pi)>0$, $\mathcal{H}(\pi/2)<0$; $\delta=0.078$, $\mathcal{H}(0)<0$, $\mathcal{H}(\pi)<0$, $\mathcal{H}(\pi/2)>0$. We can see that the curvature is negative at $k\approx 0$ in both cases. At $k\approx\pi$, and $k\approx\pi/2$ the curvature could be either positive or negative depending on δ.

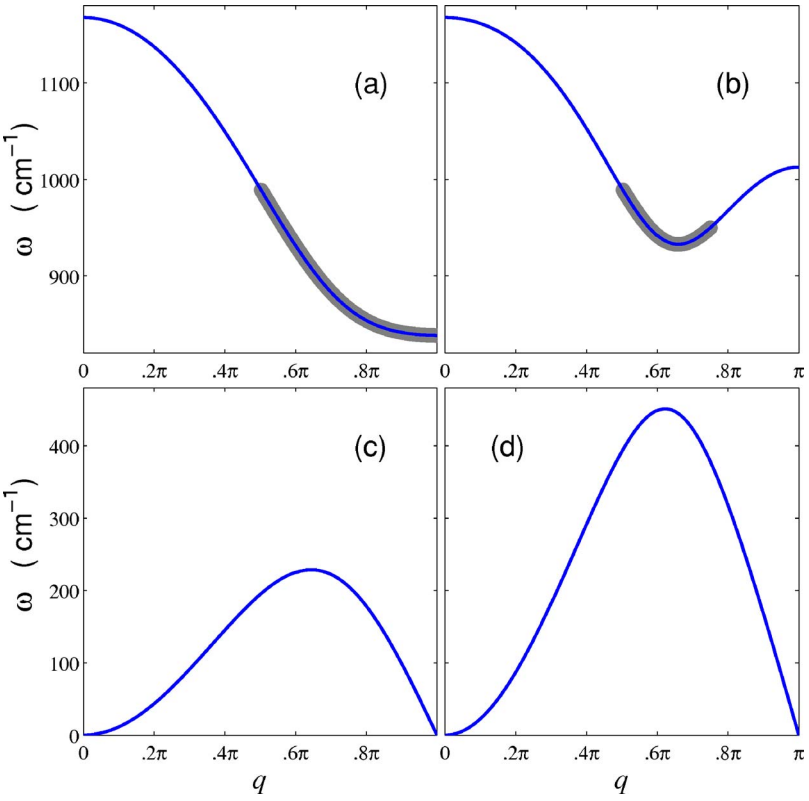

FIG. 1. (Color online) Dispersion curves: optic (a), (b) and acoustic (c), (d) branches for $\delta=0.019$ (a), (c) and for $\delta=0.078$ (b), (d) (parameter $C_2=\delta C_1$). Thick part of the dispersion curves correspond to possible existence of the breathers.

We can see that for $k \approx 0$ the curvature is negative in both cases. For $k \approx \pi$, $k \approx \pi/2$ it could be both positive or negative depending on the magnitude of δ. The sign of the curvature determines the sign of the second spatial derivative in the final continuum equations of motion. Let us define $k_0 \in]0, \pi[$ so that the corresponding coefficient ν equals zero: $f'(k_0)=0$ (k_0 is defined only for $\delta=0.078$ because for $\delta=0.019$ parameter ν equals to zero only for the boundary values of the wave number).

V. INTRODUCTION OF MODULATING FUNCTIONS

To extend the normal modes based analysis on the nonlinear case let us introduce the slow modulating functions. We use the denotations $u_n=U$, $w_n=W$, $u_{n+1}=\tilde{U}$, $w_{n+1}=\tilde{W}$ and consider the expansions in the vicinity of an arbitrary nth particle via modulating functions U, $\tilde{U}$, W, $\tilde{W}$:

$$u_{n+m} = \cos(mk)\left[U + m\epsilon\frac{\partial U}{\partial \xi} + \frac{1}{2}m^2\epsilon^2\frac{\partial^2 U}{\partial \xi^2}\right] + \sin(mk)\left[\tilde{U} + m\epsilon\frac{\partial \tilde{U}}{\partial \xi} + \frac{1}{2}m^2\epsilon^2\frac{\partial^2 \tilde{U}}{\partial \xi^2}\right] + \cdots, \tag{12}$$

$$w_{n+m} = \cos(mk)\left[W + m\epsilon\frac{\partial W}{\partial \xi} + \frac{1}{2}m^2\epsilon^2\frac{\partial^2 W}{\partial \xi^2}\right] + \sin(mk)\left[\tilde{W} + m\epsilon\frac{\partial \tilde{W}}{\partial \xi} + \frac{1}{2}m^2\epsilon^2\frac{\partial^2 \tilde{W}}{\partial \xi^2}\right] + \cdots, \tag{13}$$

where small parameter ϵ characterizes the distance between particles in the units $\xi=\varepsilon^{-1}z/l_z$, and z is dimensional distance, $m=1,2,\ldots$.

In the same way we consider the expansions in the vicinity of the $(n+1)$-th particle

$$u_{n+1+m} = \sin(-mk)\left[U + m\epsilon\frac{\partial U}{\partial \xi} + \frac{1}{2}m^2\epsilon^2\frac{\partial^2 U}{\partial \xi^2}\right] + \cos(mk)\left[\tilde{U} + m\epsilon\frac{\partial \tilde{U}}{\partial \xi} + \frac{1}{2}m^2\epsilon^2\frac{\partial^2 \tilde{U}}{\partial \xi^2}\right] + \cdots, \tag{14}$$

$$w_{n+1+m} = \sin(-mk)\left[W + m\epsilon\frac{\partial W}{\partial \xi} + \frac{1}{2}m^2\epsilon^2\frac{\partial^2 W}{\partial \xi^2}\right] + \cos(mk)\left[\tilde{W} + m\epsilon\frac{\partial \tilde{W}}{\partial \xi} + \frac{1}{2}m^2\epsilon^2\frac{\partial^2 \tilde{W}}{\partial \xi^2}\right] + \cdots. \tag{15}$$

Expansions should be considered in the vicinities of two particles because of double degeneracy of linear normal modes, except for those at the boundary of the first Brilluoin zone. By substituting the modulating functions in linearized equations (7) for u_n, u_{n+1}, w_n, w_{n+1} we obtain four partial differential equations that take into account linear parts of the equations for normal modes modulations. These equations have to be in accordance with foregoing dispersion relations. In the particular case $k=\pi/2$ the linearized equations are

$$\frac{\partial^2 U}{\partial t^2} - 2(C_1c^2 + 4C_2s^2)\epsilon\frac{\partial \tilde{U}}{\partial \xi} - 4csC_2\epsilon\frac{\partial W}{\partial \xi} - 4C_2s^2\epsilon^2\frac{\partial^2 U}{\partial \xi^2} + sc(2C_2 + C_1)\epsilon^2\frac{\partial^2 \tilde{W}}{\partial \xi^2} + 2(c^2C_1 + 2s^2C_2)U + 2sc(2C_2 - C_1)\tilde{W} = 0, \tag{16}$$

$$\frac{\partial^2 W}{\partial t^2} - 2C_1s^2\epsilon\frac{\partial \tilde{W}}{\partial \xi} + 4csC_2\epsilon\frac{\partial U}{\partial \xi} + 4C_2c^2\epsilon^2\frac{\partial^2 W}{\partial \xi^2} + sc(2C_2 - C_1)\epsilon^2\frac{\partial^2 \tilde{U}}{\partial \xi^2} + 2(s^2C_1 + 2c^2C_2)W + 2sc(2C_2 - C_1)\tilde{U} = 0, \tag{17}$$

$$\frac{\partial^2 \tilde{U}}{\partial t^2} + 2(C_1c^2 + 4C_2s^2)\epsilon\frac{\partial U}{\partial \xi} + 4scC_2\epsilon\frac{\partial \tilde{W}}{\partial \xi} - 4C_2s^2\epsilon^2\frac{\partial^2 \tilde{U}}{\partial \xi^2} + sc(2C_2 - C_1)\epsilon^2\frac{\partial^2 W}{\partial \xi^2} + 2(c^2C_1 + 2s^2C_2)\tilde{U} + 2sc(2C_2 - C_1)W = 0, \tag{18}$$

$$\frac{\partial^2 \tilde{W}}{\partial t^2} + 2C_1s^2\epsilon\frac{\partial W}{\partial \xi} - 4csC_2\epsilon\frac{\partial \tilde{U}}{\partial \xi} + 4C_2c^2\epsilon^2\frac{\partial^2 \tilde{W}}{\partial \xi^2} + sc(2C_2 - C_1)\epsilon^2\frac{\partial^2 U}{\partial \xi^2} + 2(s^2C_1 + 2c^2C_2)\tilde{W} + 2sc(2C_2 - C_1)U = 0. \tag{19}$$

Substitution of Eqs. (12)–(15), into nonlinear equations (7) leads to four nonlinear partial differential equations (NPDEs) for the functions W, $\tilde{W}$, U, $\tilde{U}$. To reduce the order of this system, one can express the functions U, $\tilde{U}$ via W, $\tilde{W}$ (see the Appendix). At this step, one can notice that for $k=\pi/2$ or $k=k_0$ the displacements u_n and w_n have the same order: we have strongly coupled longitudinal and transversal motions. Measuring the length in terms of l_z we have $k \sim \pi/2$: $u_n \sim w_n$. For the case of strong coupling, the relations can be written as

$$U = A_1W + A_2\tilde{W} + \mathcal{F}_{12}(W,\tilde{W}) + \mathcal{F}_{13}(W,\tilde{W}) + A_3\epsilon\frac{\partial W}{\partial \xi} + A_4\epsilon\frac{\partial \tilde{W}}{\partial \xi} + A_5\epsilon^2\frac{\partial^2 W}{\partial \xi^2} + A_6\epsilon^2\frac{\partial^2 \tilde{W}}{\partial \xi^2} + \cdots, \tag{20}$$

$$\tilde{U} = B_1 W + B_2 \tilde{W} + \mathcal{F}_{22}(W,\tilde{W}) + \mathcal{F}_{23}(W,\tilde{W}) + B_3 \epsilon \frac{\partial W}{\partial \xi} + B_4 \epsilon \frac{\partial \tilde{W}}{\partial \xi} + B_5 \epsilon^2 \frac{\partial^2 W}{\partial \xi^2} + B_6 \epsilon^2 \frac{\partial^2 \tilde{W}}{\partial \xi^2} + \cdots, \tag{21}$$

with $\mathcal{F}_{ij}, (i=1,2)$ of degree j in $W, \tilde{W}$; A_k, B_k $(k=1,\ldots,6)$ are given constants. In Eqs. (20) and (21), and in the following we denote by dots the terms which correspond to order higher than two by parameter ϵ in final complex equations of motion (45) and (46).

For example, if $k=\pi/2$, we have

$$A_1 = 0, \quad A_2 = -\frac{c}{s}, \quad \mathcal{F}_{12}(W,\tilde{W}) = D(W^2 + \tilde{W}^2),$$

$$B_2 = 0, \quad B_1 = -\frac{c}{s}, \quad \mathcal{F}_{22}(W,\tilde{W}) = -D(W^2 + \tilde{W}^2),$$

$$D = \frac{3cq\rho_0 C_1}{2s^4(C_1 - 2C_2)}. \tag{22}$$

For $k=0$ or $k=\pi$, degeneracy of order occurs: u or w displacements dominate. We have $k\sim 0$: $u_n \sim k w_n \sim \varepsilon w_n$. We suppose that $k\sim\varepsilon \ll 1$, $k\sim\pi$: $w_n \sim (\pi - k)u_n \sim \varepsilon u_n$. Then the modulating functions introduced in the equations for u_n and w_n provide only two NPDEs. In these two particular cases, one needs only to consider the equation for u_n (or w_n, respectively). The relations connecting u_n and w_n are obtained in the form

$$u_n = U = \varepsilon\left[\frac{c}{s}\frac{\partial W}{\partial \xi} + \frac{c}{\rho_0 s^2}(2 - 3c^2 + 3s^2\rho_0 q - 8\delta s^2)W^2\right] + \cdots \tag{23}$$

for $k=0$ and

$$w_n = W = -\frac{sc}{2}\frac{1 - 4\delta}{4\delta s^2 + c^2}\varepsilon\frac{\partial U}{\partial \xi} + \cdots \tag{24}$$

for $k=\pi$.

VI. NONLINEAR PARTIAL EQUATIONS

Let us introduce the new non-dimensional time by relation $\tau=\Omega t$, where Ω is the linear frequency for the normal mode under consideration. Substituting the expressions (20) and (21) into equations for W and $\tilde{W}$, one can obtain the corresponding NPDE for modulating functions

$$\frac{\partial^2 W}{\partial \tau^2} + \frac{f'(k)}{\Omega^2}\epsilon\frac{\partial \tilde{W}}{\partial \xi} - \frac{f''(k)}{\Omega^2}\epsilon^2\frac{\partial^2 W}{\partial \xi^2} + W + \frac{1}{\Omega^2}[D_1 W^2 + D_2 W\tilde{W} + D_3\tilde{W}^2 + D_4 W^3 + D_5 W^2\tilde{W} + D_6 W\tilde{W}^2 + D_7\tilde{W}^3] + \cdots = 0, \tag{25}$$

TABLE II. Values of constants D_j, $j=1,\ldots,7$ for $k=\pi/2$ and numerical values for $k=k_0$, corresponding to $\varepsilon=0.05$.

j	$k=\pi/2$	$k=k_0$
1	$(C_1-2C_2)Dcs/C_1$	2.25
2	0	−5.74
3	$(C_1-2C_2)Dcs/C_1$	2.57
4	$-D(3C_1q\rho_0+C_1-2C_2)/C_1$	1.89
5	$D(3C_1q\rho_0+C_1-2C_2)/C_1$	−1.14
6	$-D(3C_1q\rho_0+C_1-2C_2)/C_1$	2.42
7	$D(3C_1q\rho_0+C_1-2C_2)/C_1$	−1.14

$$\frac{\partial^2 \tilde{W}}{\partial \tau^2} - \frac{f'(k)}{\Omega^2}\epsilon\frac{\partial W}{\partial \xi} - \frac{f''(k)}{\Omega^2}\epsilon^2\frac{\partial^2 \tilde{W}}{\partial \xi^2} + \tilde{W} + \frac{1}{\Omega^2}[-D_3 W^2 - D_2 W\tilde{W} - D_1\tilde{W}^2 + D_7 W^3 + D_6 W^2\tilde{W} + D_5 W\tilde{W}^2 + D_4\tilde{W}^3] + \cdots = 0, \tag{26}$$

where D_j, $j=1,\ldots,7$ are constants depending on C_1, C_2, ρ_0, q, θ_0 (see Table II). Because of the complexity of general expressions they are given here only for $k=\pi/2$. The numerical values for $k=k_0$ are given in the rescaled dimensionless form that corresponds to $\varepsilon=0.05$.

Because of the degeneracy of either case $k=0$ or $k=\pi$, the equation for w_n leads to

$$\frac{\partial^2 \tilde{W}}{\partial \tau^2} - \lambda_1\varepsilon^2\frac{\partial^2 \tilde{W}}{\partial \xi^2} + \tilde{W} + \alpha_2\tilde{W}^3 + \cdots = 0,$$

$$\lambda_1 = \frac{C_1\cos(\theta_0) + 4c^2C_2}{4s^2C_1},$$

$$\alpha_2 = \frac{1}{\rho_0^2}\left[2(5c^2 - 4)c^2/s^2 + \frac{14}{3}\rho_0^2 q^2 s^2 - 12\rho_0 q c^2 + 32\delta c^2\right] \tag{27}$$

for $k=0$ and

$$\frac{\partial^2 \tilde{U}}{\partial \tau^2} - \lambda_2\epsilon^2\frac{\partial^2 \tilde{U}}{\partial \xi^2} + \tilde{U} + \alpha_1\tilde{U}^2 + \alpha_2\tilde{U}^3 + \cdots = 0,$$

$$\lambda_2 = -\frac{C_1\cos(\theta_0)c^2 + 20c^2s^2C_2}{4(c^2 + 4s^2\delta)^2},$$

$$\alpha_1 = \frac{3}{c}\frac{c^2(s^2 - c^2q\rho_0) + 4s^2(1 - 4c^2)\delta}{c^2 + 4s^2\delta},$$

$$\alpha_2 = -\frac{2[3c^2s^2(5c^2-1)+18c^4s^2q\rho_0-7c^6q^2\rho_0^2-12\delta s^2(48c^4-24c^2+1)]}{3c^2(c^2+4s^2\delta)}, \tag{28}$$

for $k=\pi$.

In the last NPDEs the nonlinear terms that include spatial derivatives can be neglected because of their higher orders in ϵ. All NPDEs have been given in dimensional form. They could be rescaled using characteristic physical values of different variables, e.g., changing U, $\tilde{U}$, W, $\tilde{W}$ by $\varepsilon\rho_0 U$, $\varepsilon\rho_0\tilde{U}$, $\varepsilon\rho_0 W$, $\varepsilon\rho_0\tilde{W}$. This procedure will be presented below for numerical applications in the cases $k\approx 0$, $k\approx\pi$, and $k=k_0$. Such rescaling makes the nonlinear terms and terms containing second spatial derivatives comparable.

VII. TRANSITION TO COMPLEX VARIABLES

Equation (28) can be rewritten as a first order in time PDE using the following substitution:

$$k\sim 0,\quad \Psi(\xi,\tau)=(W'+iW),\quad \Psi^\star(\xi,\tau)=(W'-iW),$$

$$k\sim\pi,\quad \Psi(\xi,\tau)=(U'+iU),\quad \Psi^\star(\xi,\tau)=(U'-iU),$$

$$k\sim\pi/2 \text{ or } k_0,\quad \begin{cases}\Psi_1(\xi,\tau)=(W'+iW), & \Psi_1^\star(\xi,\tau)=(W'-iW),\\ \Psi_2(\xi,\tau)=(\tilde{W}'+i\tilde{W}), & \Psi_2^\star(\xi,\tau)=(\tilde{W}'-i\tilde{W}).\end{cases} \tag{29}$$

We obtain two NPDEs ($k=0$)

$$-i\frac{\partial\Psi}{\partial\tau}=\Psi-\frac{\lambda_1}{2}\epsilon^2\frac{\partial^2}{\partial\xi^2}(\Psi-\Psi^\star)-\frac{\alpha_2}{8}(\Psi-\Psi^\star)^3+\cdots,$$

conjugate equation, (30)

and $k=\pi$

$$-i\frac{\partial\Psi}{\partial\tau}=\Psi-\frac{\lambda_2}{2}\epsilon^2\frac{\partial^2}{\partial\xi^2}(\Psi-\Psi^\star)-\frac{i\alpha_1}{4}(\Psi-\Psi^\star)^2-\frac{\alpha_2}{8}(\Psi-\Psi^\star)^3+\cdots$$

conjugate equation. (31)

In general case one can obtain four NPDEs, e.g., for $k=\pi/2$ their linear part is

$$-i\frac{\partial\Psi_1}{\partial\tau}=\Psi_1+\frac{f'(k)}{\Omega^2}\epsilon\frac{\partial^2}{\partial\xi^2}(\Psi_2-\Psi_2^\star)-\frac{f''(k)}{\Omega^2}\epsilon^2\frac{\partial^2}{\partial\xi^2}(\Psi_1-\Psi_1^\star),$$

conjugate equation,

$$-i\frac{\partial\Psi_2}{\partial\tau}=\Psi_2-\frac{f'(k)}{\Omega^2}\epsilon\frac{\partial^2}{\partial\xi^2}(\Psi_1-\Psi_1^\star)-\frac{f''(k)}{\Omega^2}\epsilon^2\frac{\partial^2}{\partial\xi^2}(\Psi_2-\Psi_2^\star),$$

conjugate equation. (32)

Let us introduce the change of variables

$$\tau_0=\tau,\quad \tau_1=\varepsilon\tau_0,\quad \tau_2=\varepsilon^2\tau_0,\ldots. \tag{33}$$

Setting $\psi=\phi e^{i\tau}$ (for $k=0,\pi$) and $\psi_j=\phi_j e^{i\tau}$, $j=1,2$ (for $k=\pi/2$) we further use the series

$$\phi=\varepsilon(\phi_0+\varepsilon\phi_1+\varepsilon^2\phi_2+\cdots) \tag{34}$$

and, respectively,

$$\phi_j=\varepsilon(\phi_{j0}+\varepsilon\phi_{j1}+\varepsilon^2\phi_{j2}+\cdots). \tag{35}$$

For the terms at ε^0 we have

$$k=0:\ -i\frac{\partial\phi_0}{\partial\tau_0}=0, \tag{36}$$

$$k=\pi:\ -i\frac{\partial\phi_0}{\partial\tau_0}=0, \tag{37}$$

$$k=k_0:\ -i\frac{\partial\phi_{10}}{\partial\tau_0}=0,\quad -i\frac{\partial\phi_{20}}{\partial\tau_0}=0. \tag{38}$$

This means that for $k=0$, π, $\phi_0=\phi_0(\xi,\tau_1,\tau_2)$ and for $k=k_0$, $\phi_{1,0}=\phi_{1,0}(\xi,\tau_1,\tau_2)$, $\phi_{2,0}=\phi_{2,0}(\xi,\tau_1,\tau_2)$. In the case $k=\pi/2$ the presence of first space derivatives leads to a different problem.

The terms at ε^1 are as follows:

$$k=0,\pi:\ \frac{\partial\phi_1}{\partial\tau_0}+\frac{\partial\phi_0}{\partial\tau_1}=0, \tag{39}$$

$$k=k_0:\ \frac{\partial\phi_{1,1}}{\partial\tau_0}+\frac{\partial\phi_{1,0}}{\partial\tau_1}=0, \tag{40}$$

$$\frac{\partial\phi_{2,1}}{\partial\tau_0}+\frac{\partial\phi_{2,0}}{\partial\tau_1}=0. \tag{41}$$

Conditions of resonances absence lead to equations:

TABLE III. Values of α, β versus δ for $k\sim 0$ or π.

k	δ	α	β
0	0.019	0.053	−0.07
0	0.078	0.054	−0.05
π	0.019	0.035	0.021
π	0.078	0.033	−0.23

$$k = 0, \pi: \ \frac{\partial \phi_0}{\partial \tau_1} = 0, \tag{42}$$

$$k = k_0: \ \frac{\partial \phi_{1,0}}{\partial \tau_1} = 0, \quad \frac{\phi_{2,0}}{\partial \tau_1} = 0. \tag{43}$$

Therefore $\phi_0 = \phi_0(\xi, \tau_2, \tau_3, \ldots)$ for $k = 0, \pi$ as in the case $k = k_0$, we can write that $\phi_{j,0} = \phi_{j,0}(\xi, \tau_2, \ldots)$, $j = 1, 2$.

For the terms at ε^2, conditions of resonances absence lead in the main approximation to the final complex equations

$$k = 0, \pi: \ -i\frac{\partial \phi_0}{\partial \tau_2} + \beta \frac{\partial^2 \phi_0}{\partial \xi^2} + \alpha |\phi_0|^2 \phi_0 = 0,$$

$$k = 0: \ \alpha = -\frac{3\alpha_2}{8}, \quad \beta = \lambda_1/2,$$

$$k = \pi: \quad \alpha = -\frac{3\alpha_2}{8} + \frac{5\alpha_1^2}{12}, \quad \beta = \lambda_2/2. \tag{44}$$

These are the nonlinear Schrödinger equations (NSEs) for $k = 0$ and $k = \pi$, respectively.

For $k = k_0$ the resonant equations have the general form

$$-i\frac{\partial \phi_{1,0}}{\partial \tau_2} - \frac{\lambda_2}{2}\frac{\partial^2 \phi_{10}}{\partial \xi^2} + P_1 |\phi_{10}|^2 \phi_{10} + P_2 |\phi_{10}|^2 \phi_{20} + P_5 |\phi_{20}|^2 \phi_{10} + P_6 |\phi_{20}|^2 \phi_{20} + P_4 \phi_{10}^2 \overline{\phi_{20}} + P_5 \phi_{20}^2 \overline{\phi_{10}} = 0, \tag{45}$$

$$-i\frac{\partial \phi_{2,0}}{\partial \tau_2} - \frac{\lambda_2}{2}\frac{\partial^2 \phi_{20}}{\partial \xi^2} + P_1 |\phi_{20}|^2 \phi_{20} + P_2 |\phi_{20}|^2 \phi_{10} + P_5 |\phi_{10}|^2 \phi_{20} + P_6 |\phi_{10}|^2 \phi_{10} + P_4 \phi_{20}^2 \overline{\phi_{10}} + P_5 \phi_{10}^2 \overline{\phi_{20}} = 0, \tag{46}$$

where P_i $(i = 1, 6)$ are the constants derived from NPDEs (25) and (26):

$$P_1 = \frac{3}{8}D_4 - \frac{5}{12}D_1^2 + \frac{5}{24}D_2 D_3,$$

$$P_2 = \frac{1}{8}D_5 + \frac{1}{2}D_3^2 - \frac{5}{12}D_1 D_2 + \frac{1}{12}D_2^2,$$

$$P_3 = -\frac{1}{12}D_3^2 - \frac{5}{24}D_1 D_2 + \frac{1}{8}D_2^2 + \frac{1}{8}D_5,$$

$$P_4 = -\frac{1}{24}D_1 D_2 - \frac{1}{8}D_2^2 + \frac{1}{12}D_1 D_3 + \frac{1}{4}D_2 D_3 + \frac{1}{8}D_6,$$

$$P_5 = \frac{3}{8}D_7 - \frac{5}{24}D_2 D_3 + \frac{5}{12}D_1 D_3,$$

$$P_6 = -\frac{1}{2}D_1 D_3 - \frac{1}{12}D_2^2 + \frac{1}{4}D_6 + \frac{1}{6}D_2 D_3 + \frac{1}{4}D_1 D_2.$$

TABLE IV. Values of α, β versus δ for $k \sim k_0$, $\gamma = \pm 1$.

γ	δ	α	β
+1	0.078	−0.010	0.28
−1	0.078	2.47	0.28

VIII. SOLITON-LIKE SOLUTIONS

It is known that the type of solitonlike (breather) solutions depends strongly on the signs of constants α and β in the NSE. When these signs are the same, the NSE admits the bright solitons. In the opposite case, the NSE admits "dark" solitons. From this point of view there is a significant difference between two systems of zigzag parameters introduced above. In the case $k \sim 0$ and both values of δ, parameters α and β are both negative (see Table III).

For the case ($k \sim \pi$, $\delta = 0.019$) the dispersion curve has a form similar to Fig. 1(a). In such a case both α and β are positive. Then one can obtain the envelope solitons (or breathers) as particular solutions:

$$\phi_0(\xi, \tau_2) = (2A/\alpha_s)^{1/2} \exp(iv\xi/2\sqrt{\beta_s} + i\omega\tau_2) \times \operatorname{sech}[A^{1/2}(\xi/\sqrt{\beta_s} + v\tau_2)], \tag{47}$$

where $\omega = v^2/4 - A$.

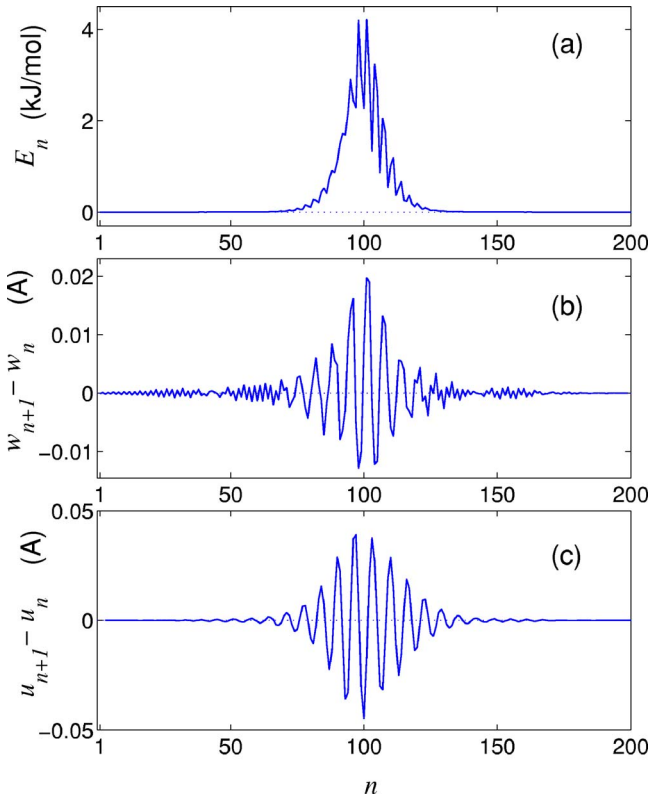

FIG. 2. (Color online) Optical breather in PE chain (parameter $\gamma = 529$ kJ/mol). The distribution along the chain of the energy E_n (a), longitudinal $w_{n+1} - w_n$ (b), and transversal $v_{n+1} - v_n$ (c) relative displacements of the chain segments is shown [breather energy $E = 56.06$ kJ/mol, frequency $\omega = 926$ cm^{-1}, velocity $s = 0.15$ (1146 m/s).

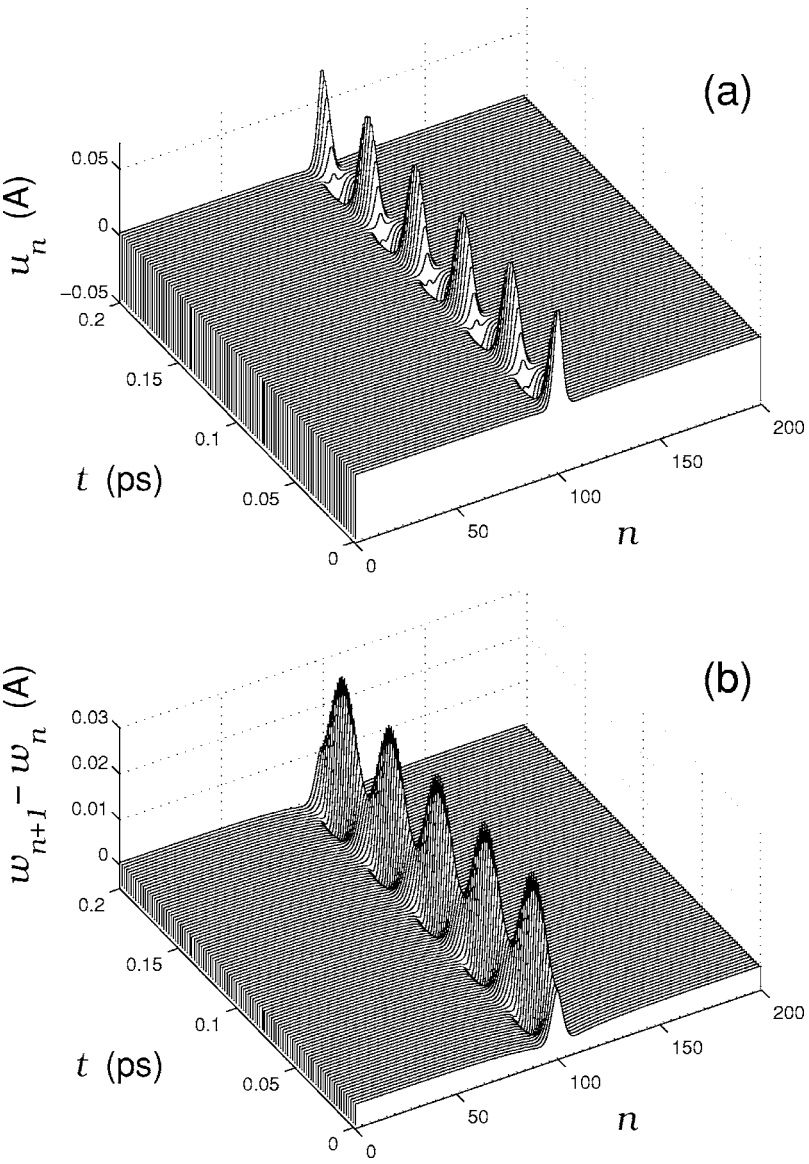

FIG. 3. Periodic change of transversal u_n and relative longitudinal displacements of zigzag $w_{n+1}-w_n$ in the localization region of optic breathers under parameters (50), $N=200$. Frequency of the breather $\omega=820.5\ \mathrm{cm}^{-1}$ is slightly lower than gap frequency.

For the second system ($k\sim\pi$, $\delta=0.078$) the dispersion curve has a form similar to Fig. 1(b) (optical branch), and dark solitons exist.

In the case $k\sim k_0$ either breather or dark soliton can exist in the vicinity of the minimal frequency. This fact has been confirmed by computer simulation (see Fig. 4). Looking for particular solutions of the form $\phi_{2,0}=\gamma\phi_{10}$, we obtain only two possible values for γ: $\gamma=\pm 1$. Then two coupled complex NPDEs (45) and (46) can be reduced to a single Schrödinger equation

$$-i\frac{\partial\phi_{1,0}}{\partial\tau_2}+\beta\frac{\partial^2\phi_{10}}{\partial\xi^2}+\alpha|\phi_{10}|^2\phi_{10}=0, \tag{48}$$

with $\beta=-\lambda_2/2$, $\alpha=P_1+P_4+P_6+\gamma(P_2+P_3+P_5)$. The values are given in Table IV. The breathers exist at $\gamma=1$ and dark solitons exist at $\gamma=-1$.

IX. NUMERICAL SIMULATIONS

In the analytical study we have made several assumptions, and now we should prove their validity. In order to do this we undertook a numerical analysis of the breathers' existence. We also determined the breathers' stability under conditions of free motion, collisions, and thermal perturbations.

For numerical modeling of breathers and their dynamics we consider the following system of equations, which corresponds to Hamilton function (3):

$$m\ddot{u}_n=-\frac{\partial H}{\partial u_n},\quad m\ddot{v}_n=-\frac{\partial H}{\partial v_n},\quad m\ddot{w}_n=-\frac{\partial H}{\partial w_n} \tag{49}$$

for $n=1,2,\ldots,N$.

We use initial conditions in agreement with approximate analytical solution. Because of some difference with the exact solution, a phonon radiation will appear. For its absorption we introduced the viscous friction at the end of the chain. As it was mentioned above, we deal with two systems of parameters for the PE crystal. One of them is[21]

$$m=14m_p,\quad p_1=8.37\ \mathrm{kJ/mol},\quad p_2=1.675\ \mathrm{kJ/mol},$$

$$p_3=6.695\ \mathrm{kJ/mol},\quad \Lambda=130.122\ \mathrm{kJ/mol},$$

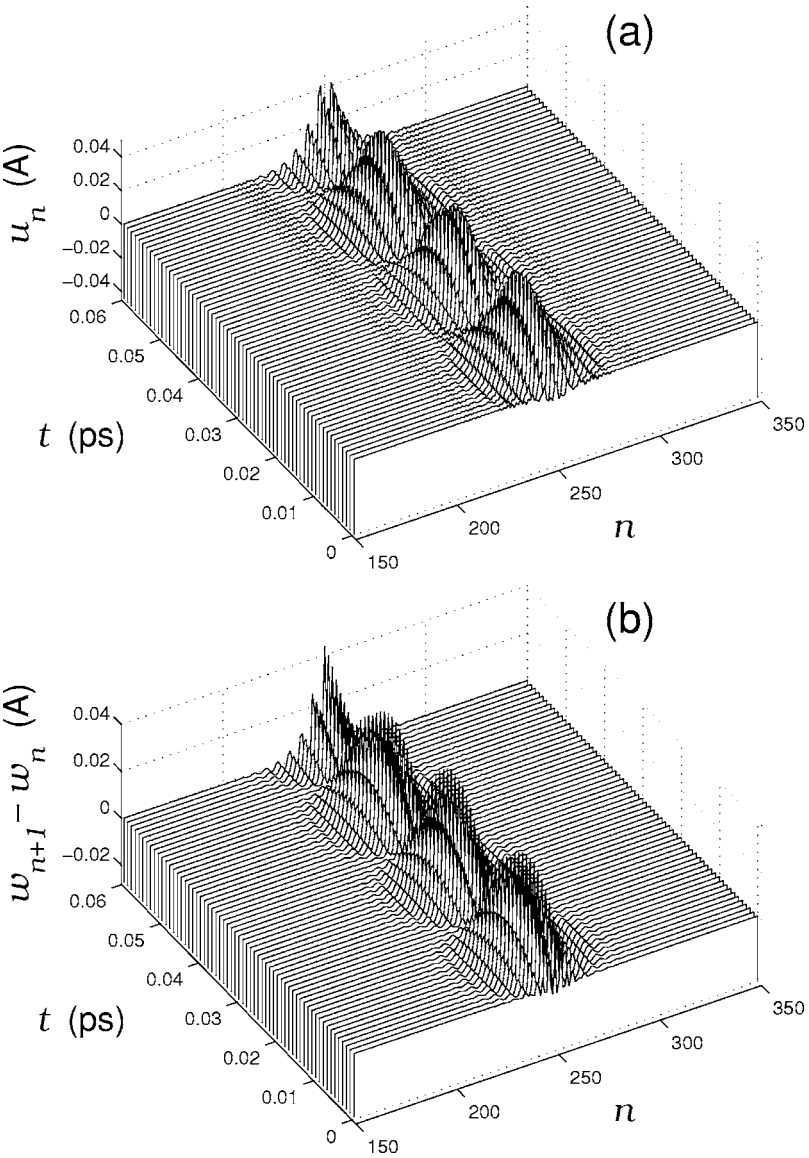

FIG. 4. Periodic change of transversal u_n and relative longitudinal displacements of zigzag chain $w_{n+1}-w_n$ in the localization region of optic breathers under parameter (51), $N=500$. Frequency of breather $\omega=928.4\ \mathrm{cm}^{-1}$ is slightly lower than frequency corresponding to low boundary of gap.

$$\theta_0 = 113\,^\circ, \quad D = 334.72\ \mathrm{kJ/mol},$$

$$q = 1.91\ \mathrm{Å}^{-1}, \quad \rho_0 = 1.53\ \mathrm{Å}, \tag{50}$$

where m_p is proton mass. Second system of parameters which is used in Ref. 22 differs with higher value of parameter

$$\Lambda = 529\ \mathrm{kJ/mol}. \tag{51}$$

For the first system of parameters a geometric nonlinearity plays a crucial role in dynamics of the PE chain. In the second case a physical nonlinearity becomes more essential. Moreover, the dispersion curves for these two cases are different. Likewise, the optical breathers also have different forms and different existence regions in the parametric space (Fig. 1). Therefore, we have to study breathers properties for both systems of parameters.

Numerical integration of equations of motion (49) has confirmed that in accordance with analytical study the optical breathers exist near low boundaries of the optical phonons frequencies for both systems of parameters (50) and (51). Typical distribution of relative displacements in the localization region of planar breather is presented in Fig. 2. Characteristics of the breathers for two cases are essentially different (see Figs. 3 and 4). In the localization regions of the breathers a local change of valence angles is accompanied by a local extension of zigzag (average values of relative longitudinal displacements $w_{n+1}-w_n$ are positive).

To consider an interaction of breathers with thermal vibrations of the chain, N_0 segments of the chain were inserted from every side into thermal bath with temperature T. Then the Langevin equations of motion are

$$m\ddot{u}_n = -\frac{\partial H}{\partial u_n} + \xi_n - \Gamma_n m\dot{u}_n,$$

$$m\ddot{v}_n = -\frac{\partial H}{\partial v_n} + \eta_n - \Gamma_n m\dot{u}_n,$$

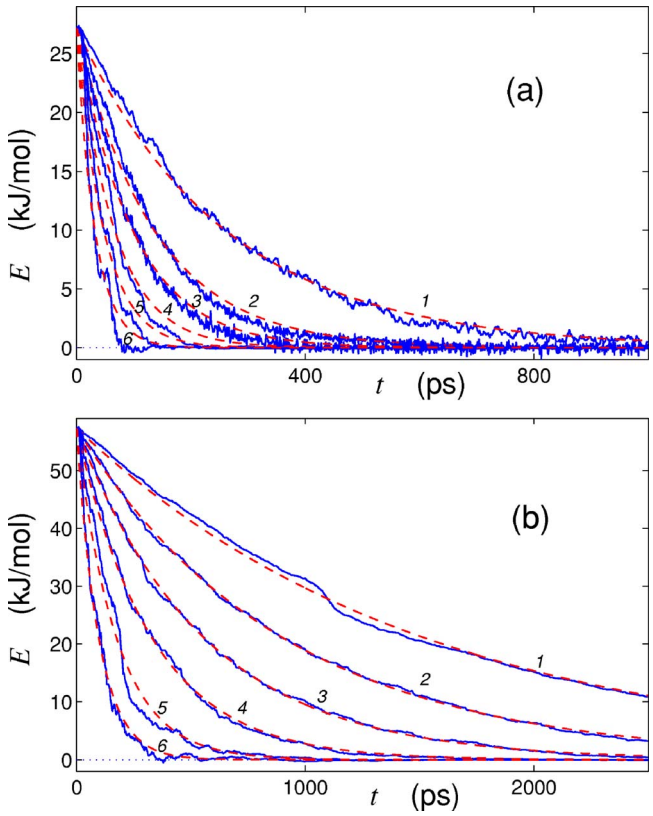

FIG. 5. (Color online) Decreasing the breather energy E in thermalized chain with $\Lambda=130.1$ kJ/mol, $\omega=820.5$ cm^{-1} (a) and $\Lambda=529$ kJ/mol, $\omega=928$ cm^{-1} (b) under temperature $T=1,2,3,5,10,20$ K (curves $1,2,\ldots,6$). Solid lines determine temporal dependencies of breather energy for concrete realization of chain thermalization, dotted lines show the corresponding exponential law $E(t)=E(0)\exp(-\alpha t)$.

$$m\ddot{w}_n = -\frac{\partial H}{\partial w_n} + \zeta_n - \Gamma_n m\dot{u}_n, \tag{52}$$

where H is the Hamiltonian function (3), ξ_n, η_n, ζ_n are random normally distributed forces that describe the interaction of nth molecule with a thermal bath, coefficient of friction Γ_n and forces ξ_n, η_n, ζ_n equal to zero for $N_0<n\le N-N_0$, and $\Gamma_n=\Gamma$ for $n\le N_0$ and $N-N_0<n\le N$.

Coefficient of friction is $\Gamma=1/t_r$, where t_r is the relaxation time of the velocity of the molecule. The random forces ξ_n, η_n, ζ_n have correlation functions

$$\langle \xi_n(t_1)\xi_l(t_2)\rangle = \langle \eta_n(t_1)\eta_l(t_2)\rangle = \langle \zeta_n(t_1)\zeta_l(t_2)\rangle = 2m\Gamma k_B T\delta_{nl}\delta(t_1-t_2),$$

$$\langle \xi_n(t_1)\eta_l(t_2)\rangle = \langle \xi_n(t_1)\zeta_l(t_2)\rangle = \langle \eta_n(t_1)\zeta_l(t_2)\rangle = 0, \quad 1\le n,l\le N_0, \quad N-N_0<n,l\le N,$$

where k_B is the Boltzmann constant and T is temperature of the heat bath.

Equations (52) were integrated numerically by the standard forth-order Runge-Kutta method with a constant step of integration Δt. The δ function was represented numerically as $\delta(t)=0$ for $|t|>\Delta t/2$ and $\delta(t)=1/\Delta t$ for $|t|\le\Delta t/2$, i.e., the step of numerical integration corresponded to the correlation time of the random force. In order to use the Langevin equation it is necessary that $\Delta t\ll t_r$. Therefore, we chose $\Delta t=0.001$ ps and relaxation time $t_r=0.1$ ps.

TABLE V. Dependence of breathers time of life t_α on the chain temperature T (frequency $\omega=820.5$ cm^{-1}, parameter $\Lambda=130.122$ kJ/mol and $\omega=928.4$ cm^{-1}, $\Lambda=529$ kJ/mol).

Λ (kJ/mol)	T (K)	1	2	3	5	10	20
130.122	t_α (ps)	180	94	68	46	33	22
529	t_α (ps)	1052	625	386	228	121	68

To avoid the friction coefficient to affect the behavior of the breather, the latter one was isolated from the heat bath by

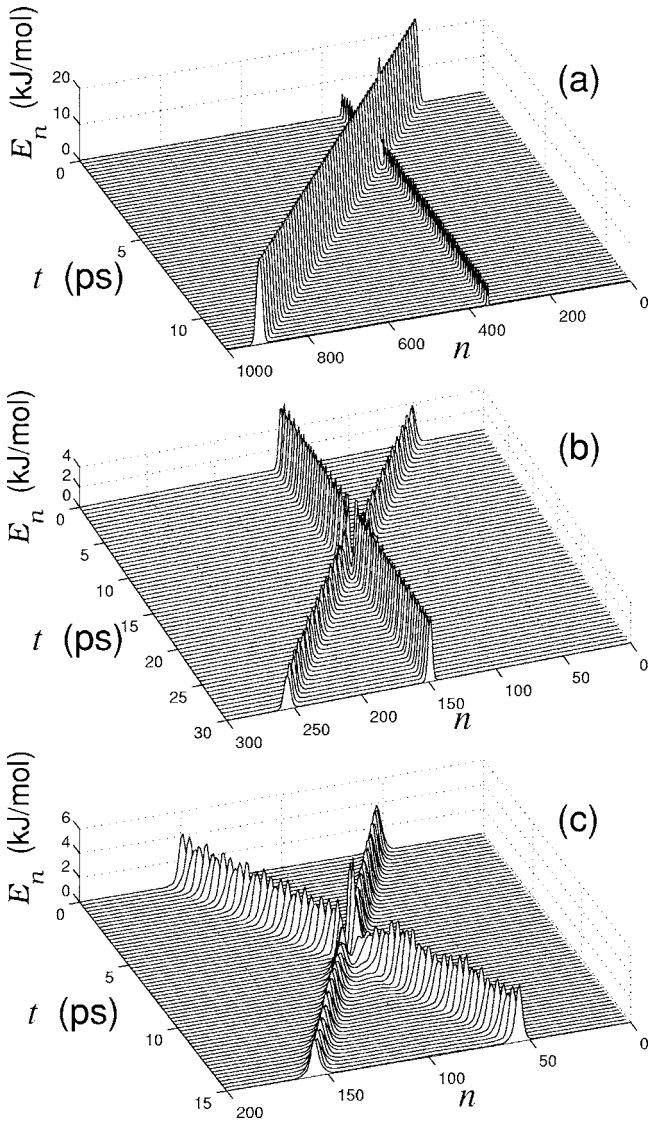

FIG. 6. Collision of supersonic acoustic soliton with stationary optic breather ($\omega=820.5$ cm^{-1}) (a), collision of the moving breather (velocity $s=0.106s_0$) with the stationary one (b), and elastic collision of two moving breathers (c). The temporal dependence of energy distribution E_n along the chain is shown. Parameters (50) has been used.

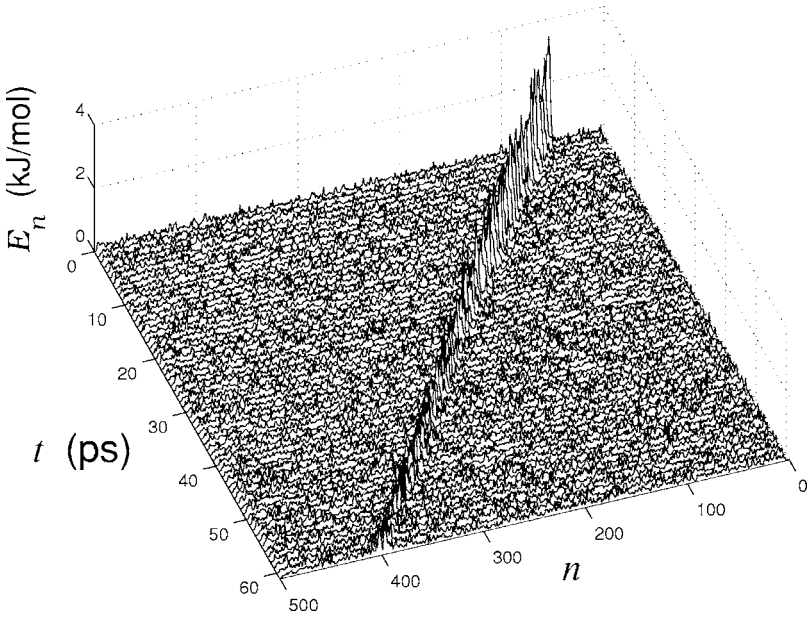

FIG. 7. Breaking of moving breather (velocity $s=0.106s_0$) in thermalized chain (temperature $T=5$ K). Temporal dependence of energy distribution along the chain E_n is shown. Parameters (50) has been used.

placing the stationary breather at the center of the chain with $N_0=50$. In this case the breather can interact only with thermal phonons arising at the ends of the chain, which are connected with heat bath. The numerical integration of the equations (52) has shown that the breathers in the thermalized chain have a finite lifetime (contrary to the isolated chain). However, the lifetime is large enough to provide a significant influence of the breathers on various physical processes.

To estimate the breather lifetime in thermalized chain let us consider the temporal dependence of the energy (Figs. 5 and 8). It is clear that the energy decreases exponentially, $E(t)=E(0)\exp(-\alpha t)$. One can determine the breather lifetime as half of breaking period $t_\alpha=\ln 2/\alpha$b $[E(t_\alpha)=E(0)/2]$. The relationship of t_α versus the chain temperature T is presented in Table V. Hence the breather lifetime is proportional to its energy-temperature ratio.

In addition to the breathers considered above, supersonic acoustic solitons may also exist in the PE chain.[19] Therefore, it is advisable to study the solitons interaction with optic breathers. We will further consider the first system of parameters only. The acoustic solitons here are caused by a local longitudinal compression of the chain (properties of the acoustic soliton were presented in Ref. 19).

Collision of the acoustic soliton with the stationary breather is shown in Fig. 6(a). It is clear that the considered interaction does not lead to a noticeable change of soliton energy, but the breather acquires a small momentum in the direction of the soliton motion. For instance, after collision with the soliton moving with velocity $s=1.024s_0$,[29] the breather with frequency $\omega=820.5$ cm^{-1} starts to move with constant velocity $s=0.0255s_0$. After each new collision the breather velocity increases and attains the limit value $s=0.106s_0$.

The motion of the breather is accompanied by a phonon irradiation with low intensity. This leads to decreasing in breather energy. We have to note that propagating breather frequency exceeds slightly the low boundary of frequency spectrum. Therefore, we deal here with the breathers in the propagation zone of optical spectrum. However, the relaxation time in this case, as well as in the case when the breather lies between acoustic and optical branches, turns out to be large enough. Actually, let us consider the collision of propagating breather ($\omega=830$ cm^{-1}) with the stationary one ($\omega=820$ cm^{-1}) [see Fig. 6(b)] and the collision of two propagating breathers ($\omega=830$ cm^{-1}) [see Fig. 6(c)]. One can see that the breathers which frequency lies in the propagation zone can move freely without any noticeable changes and can interact with similar or stationary ones as elastic particles—they exchange by the momentum without any energy decreasing.

In thermalized chain both propagating and stationary breathers have the relaxation time proportional to ratio of the energy and temperature and does not noticeably depend on the breather's velocity (Fig. 7). This time is large enough ($\sim 10^3$ periods of optical vibrations) for breathers manifestation in different physical processes.

We have shown that the optical breathers can exist both in isolated and interacting chains. The characteristics of the breathers do not depend significantly on the intermolecular interactions. In this case we can use approximation of neighbor chains being at rest.

When we take into account the interchain interaction, three types of topological solitons with topological charges $\mathbf{q}=(q_1,q_2)$ appear. Their properties are described in Ref. 23. The solutions of the first type have topological charge $\mathbf{q}=(\pm 1,0)$ and describe a localized longitudinal extension/compression of the chain by one step. The solutions of the second type have the charge $\mathbf{q}=(\pm 0.5,0.5)$ and describe a longitudinal extension/compression of the chain by half step and a twist by 180°. The solutions of the third type have the charge $\mathbf{q}=(0,1)$ and describe the twist of the chain by 360°. All these topological solutions have subsonic velocity spectra and can move without phonon irradiation.

We considered an interaction of stationary optical breather with frequency $\omega=820.5$ cm^{-1} with moving topological solitons. As it is seen from Fig. 8 such an interaction is the

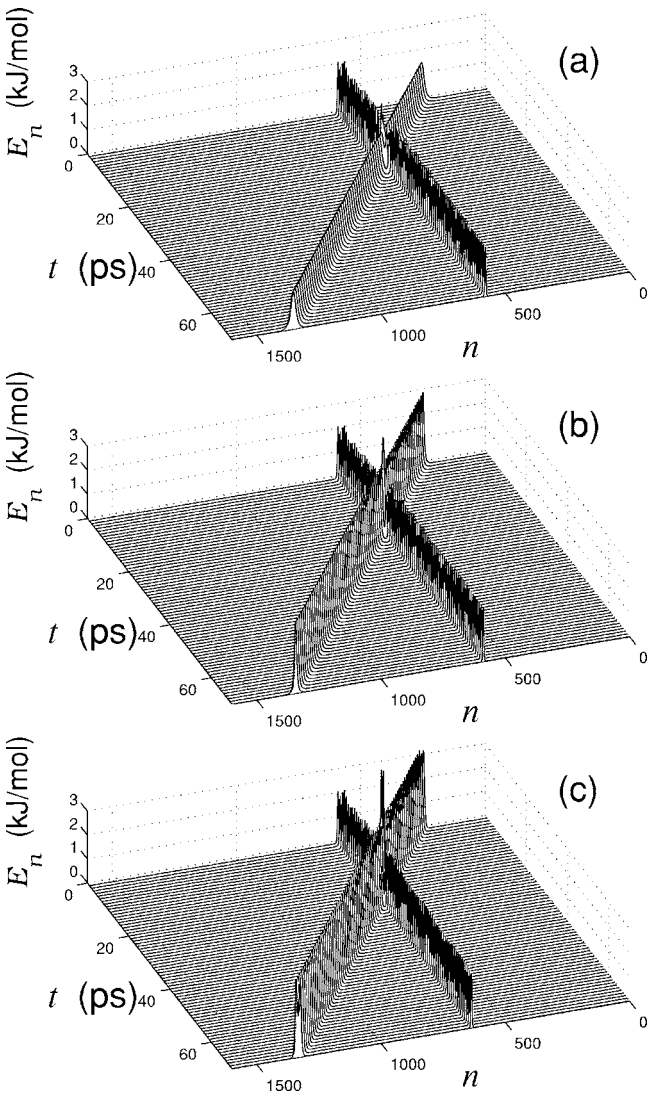

FIG. 8. Passage of topological solitons (velocity $s=0.25s_0$) with charge $\mathbf{q}=(1,0)$ (a), $\mathbf{q}=(0.5,0.5)$ (b), and $\mathbf{q}=(0,1)$ (c) through static breather (frequency $\omega=820.5$ cm^{-1}). Parameters (50) have been used.

elastic one if the first component of topological charge $q_1 \leq 0$, i.e., if a there is no compression in the localization region. In the opposite case, when $q_1<0$, the interaction with topological soliton leads to breaking the breather—see Fig. 9. Moreover, the bound state of the breather and topological soliton ($q_1>0$) may be energetically favorable. Such a coupling increases the relaxation time for the breather in thermalized chain. It was shown recently[10,27] that mutual interaction of the breathers with solitons of another type or phonons plays an important role in the heat conduction.

X. CONCLUSION

The optical breathers, which constitute the localized coupled longitudinal-transversal nonlinear excitations, can exist both in the attenuation and propagation bands of polyethylene crystal. We have obtained an approximate analytical solution for the breather using a model of isolated chain. We have numerically confirmed that taking interchain interactions into account does not lead to a significant change of the breather parameters. The reason is that the interchain interaction is somewhat weak compared to the intrachain one. We have demonstrated the breathers stability to mutual collisions. It has been shown that the presence of thermal excitations increases the breather relaxation time.

The interaction of the optical breathers with the supersonic and subsonic (topological) solitons can be either elastic or inelastic depending on the breather parameters. To the best of our knowledge, this paper presents the first analytical study of the breathers in the oscillatory chain which is different from a straight one. At the same time, we were first to investigate the mutual interactions of various types of solitons within a realistic model of the polymer chain. Both analytical and numerical results presented above provide a new insight into understanding and description of such physical processes as premelting and heat conduction in solids.

ACKNOWLEDGMENTS

The authors (L.I.M. and A.V.S.) thank the Region Rhone-Alpes and the Russian Foundation of Basic Research (Grants No. 04-02-17306 and No. 04-03-32119), respectively, for financial support.

APPENDIX

Four NPDEs with respect to modulating functions can be presented in operator form

$$L(\mathbf{X}) = \mathbf{Y}, \tag{A1}$$

where

$$\mathbf{X} = \begin{bmatrix} U \\ \tilde{U} \\ W \\ \tilde{W} \end{bmatrix}; \quad \mathbf{Y} = \begin{bmatrix} F \\ \tilde{F} \\ G \\ \tilde{G} \end{bmatrix}, \tag{A2}$$

where the left part contains only linear terms corresponding to chosen (nonperturbed) wave number and right part contains the linear terms depending on the first and second derivatives as well as the nonlinear terms till second order by ϵ inclusively.

We use further a procedure of successive approximations. The first iteration is described by the equation

$$L(\mathbf{X}) = \mathbf{0}. \tag{A3}$$

In this approximation the frequency corresponds to the nonperturbed wave number, as well as the relation between U, $\tilde{U}$

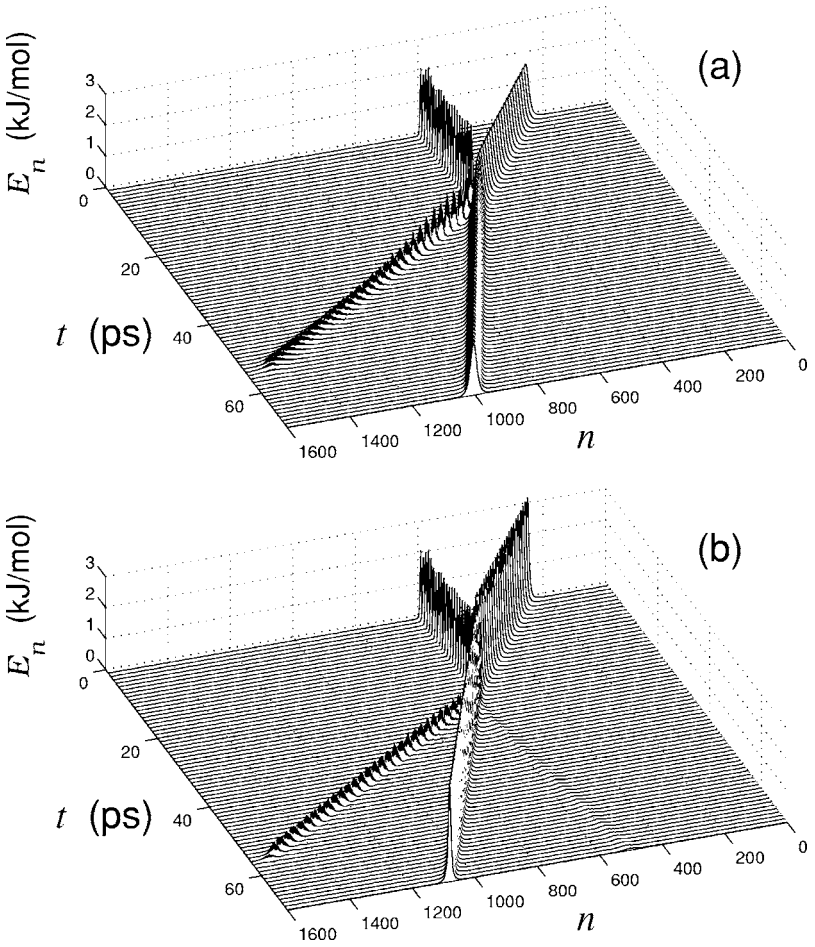

FIG. 9. Breaking of the stationary breather (frequency $\omega=820.5\ \mathrm{cm}^{-1}$) as a result of collision with topological solitons with integer charge $\mathbf{q}=(-1,0)$ (a) and half-integer charge $\mathbf{q}=(-0.5,0.5)$ (b) (velocity of topological soliton $s=0.25s_0$). Parameters (50) have been used.

and W, $\tilde{W}$. In the second approximation we substitute these relations into right part of Eq. (A1). As this takes place, the frequency in the left part corresponds to the perturbed wave number in the vicinity of chosen one. Then we can consider (A1) as linear nonhomogeneous equation with respect to U, $\tilde{U}$, W, $\tilde{W}$ in the second approximation. Its solution allows to find the relations between U, $\tilde{U}$ and W, $\tilde{W}$ until order two inclusively.

*Electronic address: lmanev@center.chph.ras.ru
†Electronic address: asavin@center.chph.ras.ru
‡Electronic address: lamarque@entpe.fr

[1] D. K. Campbell, S. Flach, and Y. S. Kivshar, Phys. Today **1**, 43 (2004).
[2] S. Aubry, Physica D **103**, 201 (1997).
[3] J. Kirkwood, J. Chem. Phys. **7**, 506 (1939).
[4] M. Magno and R. Lutz, Eur. J. Mech. A/Solids **21**, 661 (2002).
[5] J. Skinner and P. Wolynes, J. Chem. Phys. **73**, 4015 (1980).
[6] R. Boyd, Polymer **26**, 323 (1985).
[7] E. Zubova, N. Balabaev, and L. Manevitch, J. Exp. Theor. Phys. **94**, 759 (2002).
[8] V. V. Ginzburg and L. I. Manevitch, Colloid Polym. Sci. **269**, 867 (1991).
[9] O. V. Gendelman and L. I. Manevitch, Sov. Phys. JETP **75**, 271 (1992).
[10] O. V. Gendelman and A. V. Savin, Phys. Rev. Lett. **84**, 2381 (2000).
[11] H. Dvey-Aharon, P. Taylor, and A. Hopfinger, J. Appl. Phys. **51**, 5184 (1980).
[12] L. I. Manevitch, Vysokomol. Soedin. C **43**, 2215 (2001) [Polym. Sci. C **4**, 117 (2001)].
[13] L. I. Manevitch, L. Zarkhin, and N. Enikolopyan, J. Appl. Polym. Sci. **39**, 2245 (1990).
[14] V. V. Ginzburg and L. Manevitch, J. Polym. Sci. A **34**, 91 (1992).
[15] V. V. Ginzburg and L. Manevitch, J. Polym. Sci. A **34**, 98 (1992).
[16] A. I. Musienko, N. K. Balabaev, and L. I. Manevitch, Dokl. Akad. Nauk **384**, 213 (2002) [Dokl. Phys. Chem. **384**, 101 (2002)].
[17] A. I. Musienko, N. K. Balabaev, and L. I. Manevitch, Dokl. Akad. Nauk **372**, 782 (2000) [Dokl. Phys. Chem. **372**, 92 (2000)].
[18] L. V. Yakushevich, A. V. Savin, and L. I. Manevitch, Phys. Rev. E **66**, 016614 (2002).
[19] L. I. Manevitch and A. V. Savin, Phys. Rev. E **55**, 4713 (1997).
[20] N. K. Balabaev, O. V. Gendelman, and L. I. Manevitch, Phys.

Rev. E **64**, 036702 (2001).
[21] B. Sumpter, D. Noid, G. Liang, and B. Wunderlich, Adv. Polym. Sci. **116**, 27 (1994).
[22] F. Zhang, Phys. Rev. E **56**, 6077 (1997).
[23] A. V. Savin and L. I. Manevitch, Phys. Rev. B **58**, 11386 (1998).
[24] E. A. Zubova, N. K. Balabaev, L. I. Manevitch, and A. Tsyqurov, JETP **91**, 515 (2000).
[25] G. Kopidakis and S. Aubry, Physica B **296**, 237 (2001).
[26] A. V. Savin and L. I. Manevitch, Phys. Rev. B **67**, 144302 (2003).
[27] A. V. Savin and O. V. Gendelman, Phys. Rev. E **67**, 041205 (2003).
[28] L. I. Manevich and A. V. Savin, Vysokomol. Soedin. A **47**, 821 (2005) [Polym. Sci. A **47**, 499 (2005)].
[29] s_0=7790 m/s is a velocity of long wavelength optical phonons.